Analysis of Homogeneous Coplanar Strip Line

Václav ŠÁDEK, Jiří SVAČINA

Dept. of Radio Electronics, Brno University of Technology, Purkyňova 118, 612 00 Brno, Czech Republic

sadek@feec.vutbr.cz, svacina@feec.vutbr.cz

Abstract. *The goal of this work is to introduce a new, maybe complicated but in the final result mathematically simplest model of the coplanar strip line (CPS). In contrast to the usual method based on elliptical integrals the simplest circular inversion is applied. The main advantage is that our solution is mathematically less complicated but its accuracy is a little bit lower. The maximal error of the model described lies within the restricted interval between –3% and 3%. Nevertheless the final formula is useful for the practical engineering application.*

Keywords

Coplanar strips, conformal mapping, inversion, planar transmission structures, characteristic impedance.

1. Introduction

The coplanar strip line (CPS) is a member of the group of symmetrical planar microwave structures. Nowadays, when problems of leaky waves, spurious radiation and EMC of asymmetrical planar structures grow, the interest of designers has recently focused on symmetrical structures [1]. The main advantage of this type of transmission lines is that symmetrical currents mutually compensate their effects; much better than asymmetrical structures do.

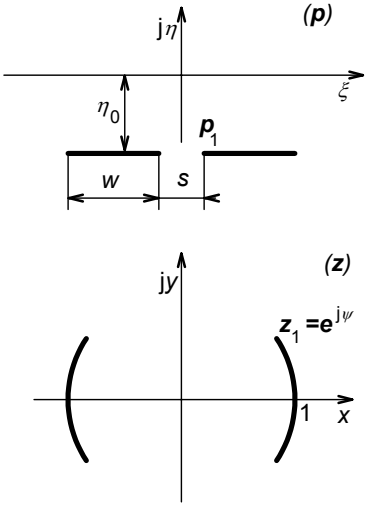

Fig. 1. The transform from the CPS to the cylindrical segments

In the article only the pure structure is analyzed. In this configuration without the dielectric substrate the CPS is not realizable. For the thick dielectric layer, in the first approach it is possible to apply the average value of permittivity below and above the CPS, but this is not accurate for the thin one. An analysis of the CPS with thin dielectric layer is now the aim of the work.

The CPS structure has already been analyzed, but the existing and often cited model [2], [3] is based on elliptical integrals. It is a very useful method, but not very practical for designers' everyday use.

One of the possibilities of simplifying the CPS model is to use another type of conformal mapping (CM). The common method is based on *Schwarz-Christoffel integral*, but there are more CMs such as the *Moebius transform* and its special form called the *circular inversion*.

2. Conformal Mapping

Let us have a CPS with the width of strips w and with the separation between them s in Gaussian plane called $\boldsymbol{p}$ at a distance η_0 (η_0 is the function of s and w) below the real axis ξ (Fig. 1) and let us define the ratio[1]

$$\kappa = (2w + s)/s \ . \tag{1}$$

Let us assume that the thickness of the electrodes is zero. The last premise is propagation of quasi-TEM wave in the CPS. Afterwards, easy CM as shown below is applicable.

The error of the method described grows with the ratio κ as shown in the end of this article and therefore it seems to be a good idea to split the analysis into two cases: one for the narrow CPS, second for the wide CPS. The border between both cases is determined from the first step of the transform as the case when angle $\psi = \pi/4$ (Fig. 2). The reason is given in the following text.

2.1 Narrow CPS

The procedure of the conformal mapping consists of two steps. The first of them is the transform of the CPS to two cylindrical segments, the second rests in their analysis.

[1] Another ratio k is used in [2] and [3]. The relation between both ratios is $k = 1/\kappa$.

The CPS placed in the position as described in the previous text, shown in Fig. 1 and called plane $\boldsymbol{p}$ is easily transformable into the cylindrical segments in plane $\boldsymbol{z}$. The relevant formula is from [4]

$$\boldsymbol{z} = 2\eta_0 / \boldsymbol{p} - \mathrm{j} \tag{2}$$

where $\eta_0 = (sw/2 + s^2/4)^{1/2}$. It is the circular inversion with the stretch and the shift in the imaginary direction. Of course this conformal transform may also be referred to as the Moebius transform in a special form.

This formula enables to determine the condition for the border between the narrow and the wide CPS based only on its own geometric parameters and not on angle ψ. The cylindrical segments cover a unit circle $|\boldsymbol{z}| = 1$, so that the end-point of the segment is $\boldsymbol{z} = \mathrm{e}^{\mathrm{j}\psi}$. Substituting this with the condition $\psi = \pi/4$ in equation (1) we get a new condition for the narrow CPS $\kappa \leq 3 + 2\sqrt{2} \approx 5.82$.

The next step is an analysis of the cylindrical segments [5]. Because of the circular symmetry of this structure, the exterior $|\boldsymbol{z}| > 1$ of the unit circle is exchangeable with its interior $|\boldsymbol{z}| < 1$. Moreover, the shape of cylindrical segments after the transform from the exterior to the interior remains absolutely identical.

This structure has two axes of symmetry, axes x and y. This fact allows analyzing only one quadrant to have a complete description of the cylindrical segments.

Therefore, only one quarter of a unit disk is analyzed (Fig. 2 plane $\boldsymbol{z}$).

The cylindrical segments analysis contains a sequence of three transforms [5] as shown in Fig. 2. The first of them is the transform $\boldsymbol{z} \rightarrow \boldsymbol{w}$ [6]

$$\boldsymbol{w} = \frac{1 + z - \sqrt{z^2 + 2z(\sin^2\varphi - \cos^2\varphi) + 1}}{2\cos\varphi}, \tag{3}$$

next $\boldsymbol{w} \rightarrow \boldsymbol{t}$

$$\boldsymbol{t} = \frac{1 + \boldsymbol{w}}{1 - \boldsymbol{w}}, \tag{4}$$

and finally $\boldsymbol{t} \rightarrow \boldsymbol{m}$

$$\boldsymbol{m} = \ln \boldsymbol{t} \tag{5}$$

where symbols $\boldsymbol{z}$, $\boldsymbol{w}$, $\boldsymbol{t}$, and $\boldsymbol{m}$ are complex variables in the planes, which are shown in Fig. 2, and φ is the angle from plane $\boldsymbol{w}$. Its magnitude is exactly $\varphi = \psi/2$. The proof is given at the end of this article in Appendix B.

The characteristic impedance of the structure in Fig. 2 in plane $\boldsymbol{m}$ is also the characteristic impedance of all other structures in Fig. 2 and also the characteristic impedance of the interior part of cylindrical segments $Z_{0\mathrm{int}}$

$$Z_{0\,\mathrm{int}} = \frac{120\pi}{\sqrt{\varepsilon_\mathrm{r}}} \frac{\alpha_1}{\pi/2} = \frac{240}{\sqrt{\varepsilon_\mathrm{r}}} \alpha_1 \tag{6}$$

where α_1 is the dimension of the structure in plane $\boldsymbol{m}$ and ε_r is the relative effective permittivity of the space inside this structure. The final form of the characteristic impedance of the narrow CPS $Z_{0\mathrm{n}}$ is given by a parallel combination of interior and exterior spaces

$$Z_{0\,\mathrm{n}} = \frac{120}{\sqrt{\varepsilon_\mathrm{r}}} \cdot \alpha_1 \,. \tag{7}$$

The point $\boldsymbol{m} = \alpha_1$ is an image of the point $\boldsymbol{t} = r_1$, which is an image of $\boldsymbol{w} = u_1$, the image of $\boldsymbol{z} = x_1 = 1$. Eqn. (3) gives

$$\begin{aligned} u_1 &= \frac{1 + x_1 - \sqrt{x_1^2 + 2x_1\left(\sin^2\varphi - \cos^2\varphi\right) + 1}}{2\cos\varphi} = \\ &= \frac{1 + 1 - \sqrt{1^2 + 2\cdot 1\left(\sin^2\varphi - \cos^2\varphi\right) + 1}}{2\cos\varphi} = \frac{1 - \sin\varphi}{\cos\varphi}, \end{aligned} \tag{8}$$

eqn. (4) yields

$$r_1 = \frac{1 + u_1}{1 - u_1} = \frac{\cos\varphi + \left(1 - \sin\varphi\right)}{\cos\varphi - \left(1 - \sin\varphi\right)} = \frac{1 + \cos\varphi}{\sin\varphi}, \tag{9}$$

and finally eqn. (5) leads to

$$\alpha_1 = \ln r_1 = \ln \frac{1 + \cos\varphi}{\sin\varphi}. \tag{10}$$

Consequently the impedance of the homogenous narrow CPS is given by the formula

$$Z_{0\mathrm{n}} = \frac{120}{\sqrt{\varepsilon_\mathrm{r}}} \ln \frac{1 + \cos\varphi}{\sin\varphi} = \frac{120}{\sqrt{\varepsilon_\mathrm{r}}} \ln r_1 \,. \tag{11}$$

The last problem, which must be solved, is the dependence of angle φ on ratio κ. The start of this problem solution consists in the definition of the ratio κ and the stretch η_0

$$\eta_0 = \sqrt{\frac{sw}{2} + \frac{s^2}{4}} = \sqrt{\frac{2w + s}{s} \cdot \frac{s^2}{4}} = \frac{s}{2}\sqrt{\kappa}\,. \tag{12}$$

Inner endpoint of CPS located in plane $\boldsymbol{p}$ ($\boldsymbol{p}_1 = s/2 - \mathrm{j}\eta_0$) transformed by the transform (2) maps itself onto the point $\boldsymbol{z}_1 = \mathrm{e}^{\mathrm{j}\psi}$ in plane $\boldsymbol{z}$. So

$$\begin{aligned} \boldsymbol{z}_1 = \mathrm{e}^{\mathrm{j}\psi} &= \cos\psi + \mathrm{j}\sin\psi = \frac{2\eta_0}{\boldsymbol{p}_1} - \mathrm{j} = \frac{s\sqrt{\kappa}}{\boldsymbol{p}_1} - \mathrm{j} = \\ &= \frac{s\sqrt{\kappa}}{\frac{s}{2}\left(1 - \mathrm{j}\sqrt{\kappa}\right)} - \mathrm{j} = \frac{2\sqrt{\kappa}}{\kappa + 1} + \mathrm{j}\frac{\kappa - 1}{\kappa + 1} \end{aligned} \tag{13}$$

and therefore

$$\tan\psi = \frac{\kappa - 1}{2\sqrt{\kappa}}\,. \tag{14}$$

Since angle φ is contained in formulas (9), (10), (11), it is necessary to recalculate the relation for $\tan\psi$ to its equivalent using angle φ. Because of the notation of r_1

$$r_1 = \frac{1 + \cos\varphi}{\sin\varphi} = \frac{1}{\sin\varphi} + \frac{1}{\tan\varphi}, \tag{15}$$

$\sin\varphi$ and $\tan\varphi$ are important for this analysis. They are

$$\tan\varphi = \frac{\sqrt{1+\tan^2\psi}-1}{\tan\psi} = \frac{\sqrt{1+\dfrac{(\kappa-1)^2}{4\kappa}}}{\dfrac{\kappa-1}{2\sqrt{\kappa}}} = \frac{\sqrt{\kappa}-1}{\sqrt{\kappa}+1}\ , \tag{16}$$

and

$$\sin\varphi = \frac{\tan\varphi}{\sqrt{1+\tan^2\varphi}} = \frac{\dfrac{\sqrt{\kappa}-1}{\sqrt{\kappa}+1}}{\sqrt{1+\left(\dfrac{\sqrt{\kappa}-1}{\sqrt{\kappa}+1}\right)^2}} = \frac{\sqrt{\kappa}-1}{\sqrt{2\kappa+2}}\ , \tag{17}$$

and both expressions (16) and (17) together with (15) give a final expression for r_1

$$r_1 = \frac{\sqrt{2\kappa+2}}{\sqrt{\kappa}-1} + \frac{\sqrt{\kappa}+1}{\sqrt{\kappa}-1} = \frac{\sqrt{\kappa}+\sqrt{2\kappa+2}+1}{\sqrt{\kappa}-1}\ , \tag{18}$$

which together with (10) and (7) leads to the final version of the characteristic impedance formula

$$Z_{0n} = \frac{120}{\sqrt{\varepsilon_r}} \cdot \ln\frac{\sqrt{\kappa}+\sqrt{2\kappa+2}+1}{\sqrt{\kappa}-1}\ . \tag{19}$$

for $\kappa \leq 5.82$ or $w/s \leq 2.41$.

2.2 Wide CPS

The error curvature of the structure in Fig. 2 grows rapidly for the wide CPS ($\kappa > 3 + 2\sqrt{2} \approx 5.82$) and simultaneously the error of the characteristic impedance (19) also grows.

There is one simple solution to this problem – simply interchange the PEC (full line) and the PMC (dashed line) in plane z. The easiest way to do it is to rotate plane z counterclockwise (multiply by complex unit j)

$$z' = \mathrm{j}z \tag{20}$$

as shown in Fig. 3.

Subsequently the analysis continues in the same way as in the case of the narrow CPS. Only the PEC and PMC are interchanged. The characteristic impedance of the interior $Z_{0\mathrm{int}}$ is in the case of the wide CPS given as

$$Z_{0\mathrm{int}} = \frac{120\pi}{\sqrt{\varepsilon_r}} \frac{\dfrac{\pi}{2}}{\alpha_1} = \frac{60\pi^2}{\sqrt{\varepsilon_r}\cdot\alpha_1}\ , \tag{21}$$

where all symbols are the same as in (6).

Because of the equivalence of the interior and the exterior of the unit disk in this case (see appendix A) the impedance of the wide CPS Z_{0w} is

$$Z_{0w} = \frac{30\pi^2}{\sqrt{\varepsilon_r}\cdot\alpha_1} = \frac{30\pi^2}{\sqrt{\varepsilon_r}\cdot\ln\dfrac{1+\cos\varphi'}{\sin\varphi'}} = \frac{30\pi^2}{\sqrt{\varepsilon_r}\cdot r_2}\ . \tag{22}$$

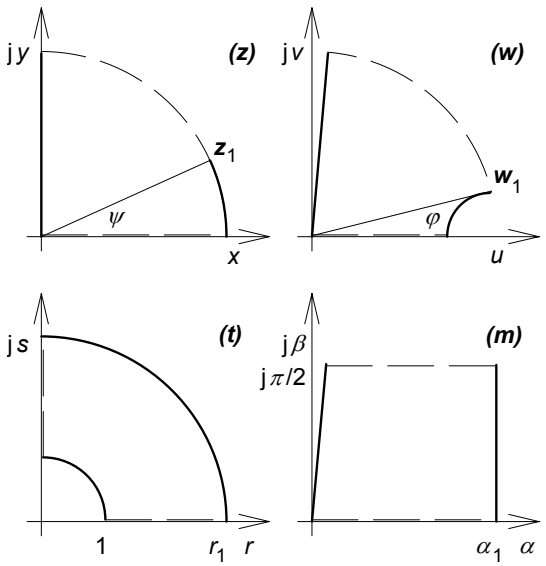

Fig. 2. The procedure of cylindrical segments analysis.

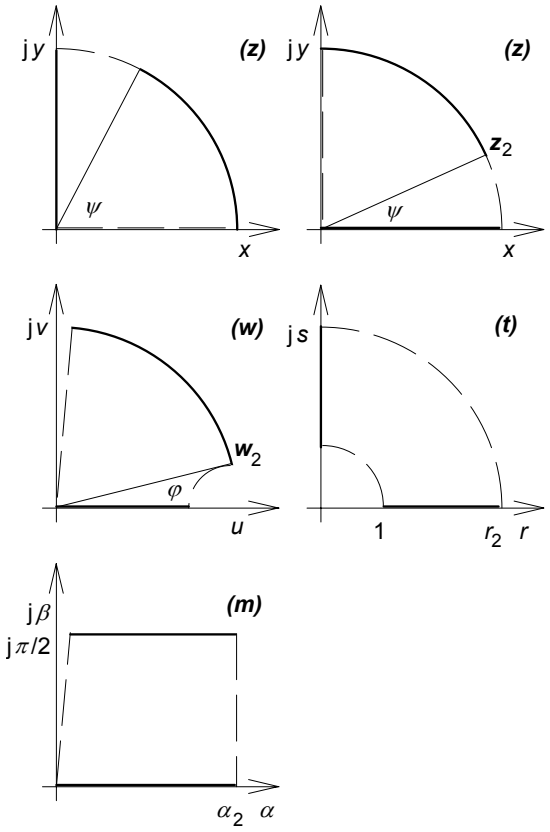

Fig. 3. The analysis of the wide coplanar strips.

The only difference is in the description of angle φ'. The auxiliary angle ψ' is complementary to angle ψ

$$\psi' = \pi/2 - \psi\ , \tag{23}$$

and therefore

$$\tan\psi' = \tan\left(\frac{\pi}{2}-\psi\right) = \frac{1}{\tan\psi} = \frac{2\sqrt{\kappa}}{\kappa-1}\ . \tag{24}$$

The next procedure is the same as in the case of narrow CPS (15) - (18). The tangent of the half argument φ' is

$$\tan\varphi' = \frac{\sqrt{1+\tan^2\psi'}-1}{\tan\psi'} = \frac{\sqrt{1+\dfrac{4\kappa}{(\kappa-1)^2}}}{\dfrac{2\sqrt{\kappa}}{\kappa-1}} = \frac{1}{\sqrt{\kappa}} \ , \tag{25}$$

and sinus of the same argument is

$$\sin\varphi' = \frac{\tan\varphi'}{\sqrt{1+\tan^2\varphi'}} = \frac{\dfrac{1}{\sqrt{\kappa}}}{\sqrt{1+\left(\dfrac{1}{\sqrt{\kappa}}\right)^2}} = \frac{1}{\sqrt{\kappa+1}} \ . \tag{26}$$

Now after repeating the technique described above we get the expression for the coordinate r_2 in plane $\boldsymbol{t}$

$$r_2 = \frac{1+\cos\varphi'}{\sin\varphi'} = \frac{1}{\sin\varphi'} + \frac{1}{\tan\varphi'} = \sqrt{\kappa+1}+\sqrt{\kappa} \ . \tag{27}$$

The characteristic impedance of the wide CPS is from (22) and (27)

$$Z_{0w} = \frac{30\pi^2}{\sqrt{\varepsilon_r}\cdot\ln\left(\sqrt{\kappa+1}+\sqrt{\kappa}\right)} \tag{28}$$

for $\kappa \geq 5{,}82$ or $w/s \geq 2{,}41$.

3. Verification

To verify the described CPS analysis [5], a simple *m-file* in *MATLAB®* was used. It is based on *the numerical Schwarz-Christoffel mapping* [7] in *SC-toolbox* [8].

```
ang=pi*i*linspace(0,90,10)/180;
pp=[0 exp(ang)];
p=polygon(pp);
for x=3:10
    f=rectmap(p,[x 11 1 2]);
    m=modulus(f);
    Z(x-2)=60*pi*m;
end;
```

A comparison of the described model and this simple model based on numerically solved conformal mapping is shown in Fig. 4. The error of the proposed method is less than 3 % for angle ψ below $\pi/4 = 45°$, where the described model works, while for greater angles ψ it grows dramatically. The cause of this error is shown in Fig. 2, planes $\boldsymbol{w}$ and $\boldsymbol{m}$ (also plane $\boldsymbol{t}$, but not visible) as additional deformation of straight borders of transformed areas. It is the visualization of the error of the transform (3).

Dividing the analyses into two parts as described above eliminates the great error for greater angles.

The whole model compound of the two submodels for the narrow CPS and for the wide ones is compared with the model described in [2] and [3]

$$Z_{0,ref} = \frac{120\pi}{\sqrt{\varepsilon_r}}\frac{\mathrm{K}(k)}{\mathrm{K}(k')} \ , \tag{29}$$

where K(k) is the complete elliptic integral of the first kind with modulus $k = 1/\kappa$. The complementary modulus is $k' = (1 - k^2)^{½}$.

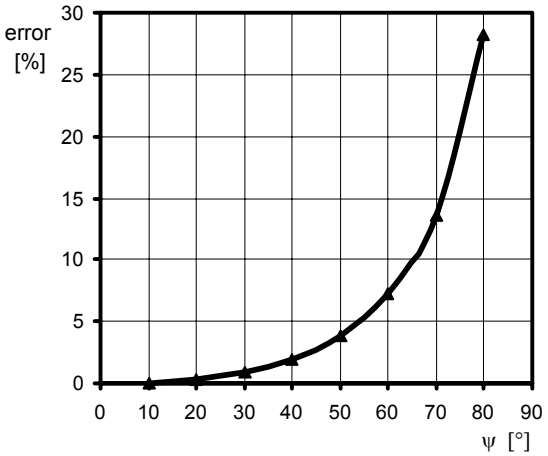

Fig. 4. The error of the CS analysis.

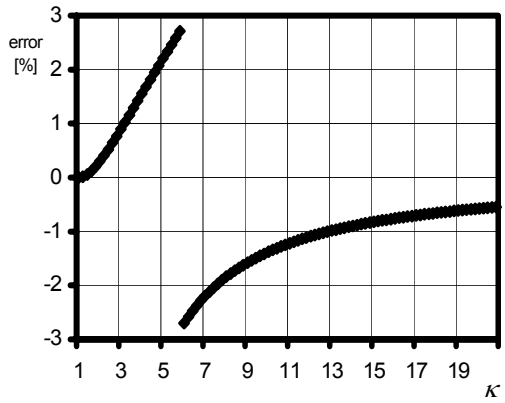

Fig. 5. The error of the described model (19) and (28) in comparison with (29).

The discontinuity in the graph of the error (Fig. 5) is due to the difference in the two submodels.

4. Discussion and Conclusion

The present work describes a new simple method for CPS analysis. Compared with the model from [3], the new model exhibits a maximum error of below 3%.

In the future the thin dielectric layer will be added under the CPS. The results of the model described here and the model with dielectric substrate will be compared with a numerical model(s) because the model [2] is only for the thick dielectric layer and as regards the model from [3] there is not information about the accuracy of the thin dielectric layer.

Our model and the used reference model from [3] are both based on conformal mapping, although each of them

in a different way. Our model so may be regarded as one of its possible alternative.

Appendix A

We prove the lemma that the interior and the exterior of the unit circle are mutually exchangeable and cylindrical segments have the same parameters for both domains.

Let us have the cylindrical segments located in plane z (see Fig. 1). Two electrodes (PEC) are situated on the circumference of the unit circle between two pairs of points, the first pair is $z_1 = e^{j\psi}$ and $z_2 = e^{-j\psi}$ and the second is $z_3 = -e^{j\psi}$ and $z_4 = -e^{-j\psi}$. After the circular inversion applied on the whole plane z

$$z^* = 1/z \ , \tag{A-1}$$

we get the plane z^*, where the unit disk from plane z is mapped onto the unit disk in plane z^*. The exterior (interior) of the disk in plane z is mapped onto the interior (exterior) in plane z^*. The end points are mapped onto

$$z_1^* = \frac{1}{z_1} = \frac{1}{e^{j\psi}} = e^{-j\psi}$$

$$z_2^* = \frac{1}{z_2} = \frac{1}{e^{-j\psi}} = e^{j\psi}$$

$$z_3^* = \frac{1}{z_3} = \frac{1}{-e^{j\psi}} = -e^{-j\psi} \tag{A-2a, b, c, d}$$

and

$$z_4^* = \frac{1}{z_4} = \frac{1}{-e^{-j\psi}} = -e^{j\psi} .$$

The points z_1^*, z_2^*, z_3^*, and z_4^* are stepwise equal to z_2, z_1, z_4 and z_3. The mapped structure in plane z^* has therefore the same shape as the cylindrical segment in plane z.

Appendix B

We prove the lemma that $\varphi = \psi/2$. The backward transform to (2) is

$$z = \frac{w - w^2 \cos\varphi}{\cos\varphi - w} . \tag{B-1}$$

The end points of the electrode in planes z and w are $w_1 = e^{j\varphi} = \cos\varphi + j\sin\varphi$ and $z_1 = e^{j\psi} = \cos\psi + j\sin\psi$. These two points are mapped onto each other; so z_{ed} on the left side of (B-1) is the product of mapping w_{ed} on the right side of (B-1)

$$\begin{aligned}
&\cos\psi + j\sin\psi = \\
&= \frac{\cos\varphi + j\sin\varphi - \cos\varphi\left(\cos\varphi + j\sin\varphi\right)^2}{\cos\varphi - \left(\cos\varphi + j\sin\varphi\right)} = \\
&= \frac{\cos\varphi + j\sin\varphi - \cos\varphi\left(\cos 2\varphi + j\sin 2\varphi\right)}{\cos\varphi - \left(\cos\varphi + j\sin\varphi\right)} = \\
&= -1 + 2\cos^2\varphi + j\frac{\cos\varphi\left(1 - \cos^2\varphi + \sin^2\varphi\right)}{\sin\varphi} = \\
&= \cos^2\varphi - \sin^2\varphi + 2j\sin\varphi\cos\varphi = \cos 2\varphi + j\sin 2\varphi
\end{aligned} \tag{B-2}$$

and this equality is possible only in the case of $\psi = 2\varphi$ or $\varphi = \psi/2$.

Acknowledgements

The research described in the paper has been prepared as part of the solution of GAČR projects No. 102/04/0553 and 102/03/H086, FRVŠ project No. 1630/2004 and with the support of the research plans MSM 262200011 and MSM 262200022.

References

[1] NAVRÁTIL V., LEONE M. The effect of differential driver asymmetries on common- and differential-mode frequency spectrum with regard to EMC. In *Proc. of the 4th International Conference of Ph.D. Students.* Miskolc (Hungary), 2003.

[2] HOFFMAN, K. *Planární mikrovlnné obvody (Planar microwave circuits).* The textbook of the Czech Technical University of Prague, Praha, 2001 (in Czech).

[3] WADELL, B.C. *Transmission line design handbook.* Boston/ London: Artech House, 1991.

[4] ŠÁDEK, V., DÝMAL, P., PROKOPEC, J., SVAČINA, J. Mapping of the coplanar strips and coplanar waveguide to the cylindrical segments. In *Elektrotechnika a informatika 2003*. Plzeň, 2003, p. 128 to 130.

[5] ŠÁDEK V., RAIDA Z., SVAČINA J. Analysis of the cylindrical segments. In *Proc. of Radioelektronika 2004*. Bratislava (Slovakia), 2004, p. 209 – 212.

[6] HENRICI, P. *Applied and computational complex analysis I. and III*. Wiley Classic Library, New York/London/Sydney/Toronto, 1988.

[7] DRISCOLL, T. A., TREFETHEN, L. N. *Schwarz-Christoffel mapping*. Cambridge Monographs on Applied and Computational Mathematics. Cambridge University Press, 2002.

[8] DRISCOLL, T. A. SC Toolbox for MATLAB, http://www.math.edu/~driscoll/SC/

[9] HLÁVKA, J., KLÁTIL, J., KUBÍK, S. *Komplexní proměnná v elektrotechnice (Complex variable in electrical engineering).* Praha: SNTL, 1990 (in Czech).

[10] REKTORYS, K. et al. *Přehled užité matematiky I, II (The compendium of the applied mathematics).* Praha: Prometheus, 2000 (in Czech).

About Authors...

Václav ŠÁDEK was born in 1977 in Hranice. He received his Ing. (MSc.) degree in Radio Electronics in 2001 at the Technical University of Brno. At present, he is a Ph.D. student at the Department of Radio Electronics of the Brno University of Technology. His research activities include the analysis of planar microwave transmission structures.

Jiří SVAČINA was born in 1948 in Nové Město na Moravě. He is currently the head of the Department of Radio Electronics, Brno University of Technology. His research activities contain microwave techniques, especially the quasistatic analysis of planar structures, and recently he has worked in the field of EMC.